ANGULAR INFORMATION RESOLUTION FROM CO-PRIME ARRAYS IN RADAR

Radmila Pribić

Sensors Advanced Developments, Thales Nederland Delft, The Netherlands

ABSTRACT

Angular resolution can be improved by using co-prime arrays instead of uniform linear arrays (ULA) with the same number of elements. We investigate how the possible co-prime angle resolution is related to the angle resolution from a full ULA of the size equal to the virtual size of co-prime arrays. We take into account not only the resulting beam width but also the fact that fewer measurements are acquired by co-prime arrays. This fact is especially relevant in compressive acquisition typical for compressive sensing. This angular resolution is called angular information resolution as it is computed from the intrinsic geometrical structure of data models that is characterized by the Fisher information. Based on this information-geometry approach, we compare angular information resolution from co-prime arrays and from the two ULAs. This novel resolution analysis is applied in a one-dimensional azimuth case. Numerical results demonstrate the suitability in radar-resolution analysis.

Index Terms**—** resolution, information geometry, co-prime arrays, compressive sensing, radar

1. INTRODUCTION

Resolution is defined by the minimum distance between two objects that still can be resolved. Besides the sensing bandwidth, the signal-to-noise ratio (SNR) is also crucial in the ability to resolve close objects (e.g.[1]). The sensing bandwidth of angle processing is given by the wavelength and the antenna aperture size: either actual as in a full uniform array or virtual as in the case of co-prime arrays. Our resolution analysis includes SNR and processing gain (PG) as being critical with the spatial acquisition of fewer samples what is typical for compressive sensing (CS).

When seeking the resolution limits, we keep exploring a practical combination of information geometry (IG) and CS in radar ([2]). IG is stochastic signal processing that treats the stochastic inferences as structures in differential geometry (e.g. [3-5]). The intrinsic geometrical structure of measurement models is conveniently characterized in terms of the Fisher information metric. Accordingly, potential resolution of sensors is based on information distances on such statistical manifolds.

When focusing on the system level, we also check how the resolution analysis suits sparse-signal processing (SSP), and provides the limits in high resolution. SSP is nowadays a major part of CS that is also optimized to information in measurements. The optimization is based on the two conditions: sparsity of processing results and the sensing incoherence (e.g. [6]). In radar, SSP can be seen as a refinement of existing processing (e.g. [7-8]). SSP is crucial in the back end of a sensor with CS, while its front end facilitates compressive acquisition of measurements. When fewer measurements are enabled already before reception as in the case of co-prime arrays, the compressive acquisition is usually called sparse sensing (e.g. [9]). Compressive acquisition makes also overall PG, certainly PG from SSP, additionally important. Optimal PG from SSP can be achieved if spatial measurements (needed for angles) are combined with temporal measurements (needed for range and doppler).

Both IG and CS have a potential to improve radar performance (and perhaps also lower the costs) because the demands of data acquisition and signal processing can be optimized to the information content in radar measurements. Our resolution analysis with IG and CS is novel, and also understood directly in practical cases.

In this paper, we focus on effects to angular resolution from fewer measurements acquired by active co-prime linear arrays (LAs). Moreover, since we keep exploring CS at the system level, we also investigate how measurements from the co-prime LAs suit SSP in the back-end.

1.1. Related Work

Information resolution has been studied (e.g. [2], [5] and [10]) but not related to co-prime arrays or compressive acquisition as typical for CS.

Sparse sensing by co-prime sampling has been studied separately in time and in space (e.g. [9]), also combined (e.g. [11]) and fully combined in radar ([12], summarized in 2.2 in this paper).

1.2. Outline and Main Contributions

In Section 2, co-prime LAs are presented in active radar with CS (as also indicated in [9]). In addition, SSP with spatial measurements from co-prime LAs is also given (as introduced in [12], with main contributions of suitability of co-prime LAs to SSP with optimal PG).

In Section 3, potential angular resolution is derived based on information distances, with main contributions of including the effects of fewer measurements from sparse sensing. In Section 4, numerical results with SSP and the resolution analysis are shown. In the end, conclusions are drawn and future work indicated.

2. CO-PRIME ARRAYS IN ACTIVE CS RADAR

In standard CS, compressive acquisition applies in the analog domain as analog-to-information conversion (AIC, e.g. [6]) after reception with a full number of antenna

978-0-9928626-3-3/15/$31.00 ©2015 IEEE

elements. In radar, such AIC causes drawbacks such as: many analog delicate computations, SNR loss, changed stochastic behavior of radar data, etc. Since all the AIC difficulties shall better be avoided, we investigate compressive acquisition before reception, i.e. sparse sensing, and moreover, try exploring the existing means in a radar system: waveforms and antenna arrays (AA) for temporal and spatial acquisition, respectively (e.g. [12]).

In this work, we keep exploring AAs for spatial sparse sensing with co-prime LAs, and focus on the angular resolution. Moreover, while focusing on the system level, we also demonstrate SSP in the back-end.

2.1. Co-prime linear arrays

Co-prime arrays are defined by a pair of uniform LAs (ULAs) formed by M and L elements and with an inter-element spacing of Ld and Md, respectively, where M and L are co-prime integers and d is a parameter usually equal to the half-wavelength ([9]). In the case of $M = 6$ and $L = 5$, the element positions of the pair of co-prime arrays are shown in Fig. 1. Due to the co-prime spatial sampling, the elements of the array coincide only at the positions that are a multiple integer of MLd, e.g. 0 and $30d$ in Fig. 1.

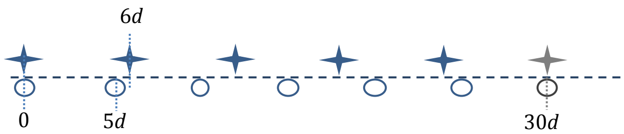

Fig. 1. Positioning of of co-prime arrays with M=6 and L=5.

A major advantage of co-prime arrays is a potential to achieve high angle resolution using a reduced number of sensors. Namely, ML beams with resolution of the order $1/ML$ can be achieved by two co-prime arrays of order M and L connected to M-point and L-point DFT filter banks generating M and L outputs, respectively (Fig.2 from [9]). Each output, defined as: $H_m(e^{j\omega}) = H\left(e^{j(\omega-2\pi m/ML)L}\right)$ and $G_l(e^{j\omega}) = G\left(e^{j(\omega-2\pi l/ML)M}\right)$, for $0 \le m \le M-1$, $0 \le l \le L-1$, and $\omega = \pi\sin\theta$, corresponds to shifted versions, in increments multiple of $2\pi/ML$, of the responses $H(e^{j\omega L})$ and $G(e^{j\omega M})$, obtained from low-pass responses with cut-off spatial frequencies π/M and π/L and decimated by a factor L and M, respectively. The product of responses at the m^{th} and l^{th} outputs:

$$F_{lm}(e^{j\omega}) = G\left(e^{j(\omega-2\pi l/ML)M}\right)H\left(e^{j(\omega-2\pi m/ML)L}\right) \quad (1)$$

for $0 \le n \le ML-1$, is characterized by a unique pass-band centered at $2\pi n/ML$ with width $2\pi/ML$. In other words, there is only one overlapping beam among the M beams of $G_l(e^{j\omega})$ and the L beams of $H_m(e^{j\omega})$, as indicated in Fig. 2. Moreover, from the ML combinations of the two responses, different ML overlapping beams are obtained, exactly as in the case of an ML DFT filter bank for an ULA with ML elements.

Measurements from co-prime receive arrays have been applied to DOA, i.e. angle (e.g. [9], [13] and [14]), or angle-frequency processing (e.g. [11]). These processing techniques are based on covariance (2nd order statistics) what is not very convenient for radar processing.

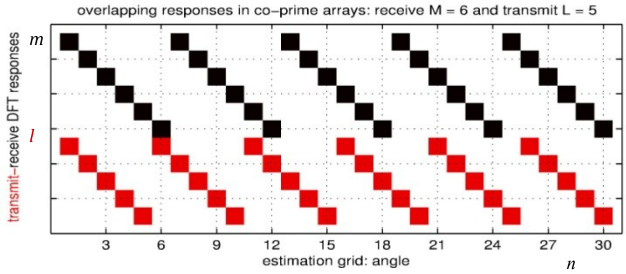

Fig. 2. Unique pairs of L transmit and M receive responses from co-prime LAs (with M=6 and L=5, Fig. 1) over ML angle cells (as in [9]). Each cell is uniquely represented by a pair (H_m, G_l), as given in (1) and utilized in (4).

2.2. SSP with co-prime AA measurements

Raw radar measurements $\boldsymbol{y}$ (e.g. [15]) can be modeled as:

$$\boldsymbol{y} = \boldsymbol{Ax} + \boldsymbol{z}\,, \quad (2)$$

by a sensing matrix $\boldsymbol{A}$, a sparse radar profile $\boldsymbol{x}$, signals $\boldsymbol{Ax}$ and a (complex Gaussian) receiver-noise vector $\boldsymbol{z}$ with zero mean and equal variances γ, $p(\boldsymbol{z}|\gamma) \propto \exp(-|\boldsymbol{z}|^2/\gamma)$. When $\boldsymbol{x}$ is sparse, the usual SSP, e.g. LASSO, applies as:

$$\boldsymbol{x}_{\text{SSP}} = \arg\min_x \{\, |\boldsymbol{y}\text{-}\boldsymbol{Ax}|^2 + \eta|\boldsymbol{x}|_1 \,\}, \quad (3)$$

with the l_1-norm $|\boldsymbol{x}|_1$ promoting the sparsity, the l_2-norm $|\boldsymbol{y}$-$\boldsymbol{Ax}|$ minimizing the noise, and a regularization parameter η that balances between the two tasks. In radar, the parameter η is closely related to the detection threshold (e.g. [7-8]). An underdetermined system can be solved i.e. M measurements in $\boldsymbol{y}$ can be enough for N outputs in $\boldsymbol{x}$, because of the sparsity, i.e. only K nonzeros in $\boldsymbol{x}$, $M < N$, $K < M$, and incoherence of $\boldsymbol{A}$ (e.g. [6]).

The basic SSP from (3) uses complex-valued measurements directly what is preferred in radar because of higher processing gain (PG, e.g. [15]). The covariance-based processing works with co-prime receive arrays leading to power-based SSP. Moreover, the covariance estimation needs training data or snapshots that are hardly available from a radar system. Finally, power-based SSP can hardly work for all radar parameters (i.e. range, doppler and angles) at once as desired for optimal PG.

Therefore, we prefer exploring transmit-receive co-prime arrays as more appropriate for active radar ([12]). As indicated in [9], with co-prime integer numbers M and L of receive and transmit elements, respectively, an outcome $C_{mn}(t)$ of an m^{th} receive filter (whose pattern is known for all ML angles, as in [9], and shown in Fig. 2), at time t and angle θ_n, $0 \le n \le ML-1$, can be modeled as:

$$C_{m,n_{ml}}(t) = \sum_{l=1}^{L} r_{n_{ml}}(t)\ \left(H_{m,n_{ml}} G_{l,n_{ml}}\right) + Z_m(t) \quad (4)$$

where $r_n(t)$ is an echo at t from θ_n, a pair (m, l) is unique for $\omega_{n_{ml}}$, $\omega_n = \pi\sin\theta_n$, (e.g. (m, l) is (1,1) for θ_1 at n =1, in Fig. 2), H_{mn} and G_{ln} are responses of the m^{th} receive, and an l^{th} transmit filter (interpreted over all ML angles, as in Fig. 2), respectively, and $Z_m(t)$ is the DFT of the noise.

The received data $C_{mn}(t)$ contain already co-prime products $H_{mn}G_{ln}$, and moreover, the temporal part $r_n(t)$ remains unchanged. Finally, we create an Nx1 data vector $\boldsymbol{c}(t)$ with $c_n(t) = \sum_{m=1}^{M} C_{mn}(t)$, being its n^{th} element.

Now we can build a model suitable for SSP, with a vector $\boldsymbol{y}(t)$ of radar measurements at ML virtual elements coming from inverse DFT of the M received data sorted in $\boldsymbol{c}(t)$, as:

$$\boldsymbol{y}(t) = \boldsymbol{F}\boldsymbol{c}(t) = \boldsymbol{F}\boldsymbol{x}(t) + \boldsymbol{z}(t), \quad (5)$$

where $\boldsymbol{c}(t)$ is the Nx1 co-prime data vector, $\boldsymbol{F}$ is an MLxN steering matrix whose n^{th} column: $vec[\boldsymbol{g}_n \boldsymbol{h}_n^T]$ at ω_n, has ML distinct (virtual) positions i, $i \in [0\ 2ML\text{-}(M{+}L)]$. The steering values: receive $h_{m,n}$ and transmit $g_{l,n}$ write as: $h_{m,n} = e^{jmL\omega_n}$ and $g_{l,n} = e^{jlM\omega_n}$, respectively. Such a steering matrix $\boldsymbol{F}$ applies also to an LA of size N.

Hence, only M received data are acquired by the AA for an Nx1 angle profile $\boldsymbol{x}(t)$, M<N, N=ML, directly with less AA elements and without AIC.

The spatial data $\boldsymbol{y}(t)$ from (5) can be extended to doppler and range by modeling $\boldsymbol{x}(t)$ over a coherent processing time t. Thus, the echo $x_n(t)$ of a target at angle θ_n, delay τ_n and doppler f_n is modeled as a replica of a (single) transmitted signal $s(t)$ shifted in time by τ_n and in frequency by f_n, and with amplitude $\alpha(\theta_n, \tau_n, f_n)$, as:

$$x_n(t) = s(t - \tau_n)\exp(j2\pi f_n t)\, \alpha(\theta_n, \tau_n, f_n) \quad (6)$$

For the simplicity, we elaborate further a range-only case in pulse radar. (The extension to doppler is straightforward.) Temporal sampling is not compressive yet but kept Nyquist in an NxN_t matrix $\boldsymbol{Y}$ of spatial measurements $\boldsymbol{y}(t)$ taken over N_t time samples, for N_τ estimates of delays via an N_τxN_t model matrix $\boldsymbol{S}$ aiming for an NxN_τ angle-range profile matrix $\boldsymbol{X}$. A data model writes as $\boldsymbol{Y} = \boldsymbol{F}\boldsymbol{X}\boldsymbol{S} + \boldsymbol{Z}$, whose vector form is suitable for SSP from (3). The model matrices $\boldsymbol{S}$ and $\boldsymbol{F}$ in the combined model are mutually incoherent by their physical nature. Namely, shifts in time and shifts in phase are correctly isolated by the physics. This also holds for shifts in frequency in the doppler matrix.

Recall that receive-receive, i.e. passive, co-prime arrays provide M+L measurements. ML products of two sums are involved in the covariance estimate, each written as: $[\sum_n r_n(t)\, h_{mn} + z_m(t)][\sum_j r_j(t)\, g_{lj} + z_l(t)]^*$. The only outcome: $\sum_n |r_n(t)|^2\, h_{mn} g_{ln}^*$, matters while many cross-terms are ignored under the assumptions of uncorrelated target echoes and i.i.d. noise. In addition, even such an ideal covariance estimate provides only $|r_n(t)|^2$, i.e. power, for temporal processing, and thus, no doppler and no coherent processing at all. Accordingly, this covariance-based SSP can hardly give as much PG as the SSP based on (3)-(6).

3. ANGULAR INFORMATION RESOLUTION

Information geometry (IG) is the study of manifolds in the parameter space of probability distributions, using the tools of differential geometry (e.g. [3-5]). These spaces are generally non-Euclidean, which basically implies that the inner product of two vectors $\boldsymbol{x}$ and $\boldsymbol{y}$: $\langle \boldsymbol{x}, \boldsymbol{y}\rangle = \boldsymbol{x}^{\mathrm{H}}\boldsymbol{y}$, is redefined as: $\langle \boldsymbol{x}, \boldsymbol{y}\rangle = \boldsymbol{x}^{\mathrm{H}}\boldsymbol{G}\boldsymbol{y}$, where $\boldsymbol{G}$ is a metric tensor defined by the Fisher information matrix in IG. The metric tensor makes the actual length of curve differ from the length in Euclidean space. The shortest path between two points is called a *geodesic* what is the extension of the notion of a straight line to non-Euclidean spaces. A clear example of a geodesic in a non-Euclidean space is the shortest path on the spherical surface. Here, straight lines do not exist: the shortest path between two points on the spherical surface is the shorter great circle arc.

We derive potential resolution based on information distances in an azimuth-only case whose measurements are acquired from different LAs. In particular, we investigate how the possible co-prime angle resolution is related to the angle resolution from a full ULA of the size M and a full ULA of the size ML.

A received signal y_i at an array-element position μ_i (measured in half-wavelength units) is modeled as:

$$y_i = \alpha\, e^{j\pi\mu_i \sin\theta} + z_i = \alpha\, e^{j\mu_i\omega} + z_i = \alpha a_i + z_i\ , \quad (7)$$

where α is a target echo, ω is the angle parameter (instead of θ, $\omega = \pi\sin\theta$ as in Section 2) and z_i is the receiver noise, i.e. complex Gaussian with zero mean and equal variances γ, $p(z_i|\gamma) \propto \exp(-|z_i|^2/\gamma)$. The target echo α is kept constant (so-called SW0 in radar, e.g. [15]). For fair comparison, we let the transmit array as well as the echo α be equal in all the three receive-array cases described as:

- ULA with M elements: $\{\mu_i\} = \{0\ 1\ ...\ M\text{-}1\}$;
- ULA with ML elements: $\{\mu_i\} = \{0\ 1\ ...\ ML\text{-}1\}$;
- co-prime *LA* with *M receive* elements: $\{\mu_i\} = \{0\ L\ 2L\ ...\ (M\text{-}1)L\}$;

The Fisher information metric $G(\omega)$ for the angle parameter ω writes as (e.g. [2] and [16]):

$$G(\omega) = -\mathrm{E}\left[\frac{\partial^2 \ln p(\boldsymbol{y}|\omega)}{\partial\omega^2}\right] = 2\frac{\alpha^2}{\gamma}\sum_i \mu_i^2 = 2\,\mathrm{SNR}\sum_i \mu_i^2 \quad . \ (8)$$

where SNR is the input SNR of a target, and $p(\boldsymbol{y}|\omega)$ is the Gaussian probability density function $p(\boldsymbol{y}|\omega)$ of a vector $\boldsymbol{y}$ of measurements from an LA given the unknown parameter ω. The second derivative used in (8), writes as:

$$\frac{\partial^2 \ln p(y_i|\omega)}{\partial\omega^2} = -2\mu_i^2(\alpha/\gamma)Re\{a_i^* y_i\} \quad ,$$

where the matched-filtering (MF) value: $a_i^* y_i$ also appears. The expected value is $-2\mu_i^2\,\alpha^2/\gamma$ as used in (8). Note in $G(\omega)$ that PG from an AA configuration comes from the sum $\sum_i \mu_i^2$, and that the edge elements contribute most.

In the accuracy analysis, the metric $G(\omega)$ is typically applied to the Cramer-Rao bound (CRB) of the mean squared error (MSE) of an unbiased estimator $\hat{\omega}$ of ω, i.e. $\mathrm{MSE}(\hat{\omega}) \geq \mathrm{CRB}(\omega) = 1/G(\omega)$ (e.g. [16]).

In the resolution analysis, information distances on this 1D statistical manifold are simply computed (e.g. [2]), as:

$$d(\omega, \omega + \delta\omega) = \int_{\omega}^{\omega+\delta\omega} \sqrt{G(\mathrm{u})}\, d\mathrm{u} = \delta\omega\sqrt{2\,\mathrm{SNR}\sum_i \mu_i^2}. \ (9)$$

Information resolution is higher if the information distance is larger. With the same separation $\delta\omega$ between two angles, the information distance differs only because of $G(\omega)$. Thus, the same information distance at $\delta\omega$ can be achieved by different LA configurations but only with appropriate input SNR. Since our goal is to assess changes in information resolution of different LAs, we compare information distances from (9). (Finding the information resolution at $\delta\omega_{min}$ from $d(\omega, \omega + \delta\omega_{min})$ at which two angles can be resolved is another goal, e.g. [2].)

4. NUMERICAL RESULTS

Numerical results on angular information resolution with co-prime LAs are given here. Moreover, while focusing on the system level, we also demonstrate SSP in the back-end.

4.1. Co-prime arrays and SSP

Angular resolution of co-prime LAs (being connected to a DFT filter bank, M=6 and L=5 as in Fig. 1) is indicated by a single beam of all the ML beam responses, in Fig. 3a. The co-prime response is comparable with the response of an ULA with ML elements (Fig. 3b). The advantages of the co-prime array solution are also clear when compared to an ULA with M receive elements, as shown in Fig. 3c.

Numerical tests with the co-prime LAs measurements from (4) demonstrate angle processing from (5), and also angle-range processing indicated in (6) in Fig. 4 and Fig. 5, respectively. SSP from (3) is performed by yall1 ([17]). In both cases, 12 nonzeros are randomly located over the estimation grid. The true amplitude α of a nonzero in $\boldsymbol{x}$ is kept constant (so-called SW0) and given by its SNR, SNR = $|\alpha|^2/\gamma$, where γ is fixed: γ=1. A realistic case of range processing in pulse radar is merged with the angle processing. The N_txN_τ sensing matrix $\boldsymbol{S}$ contains delayed replicas of a transmitted pulse that is a linearly frequency modulated (LFM) waveform, with the bandwidth equal to the sampling frequency.

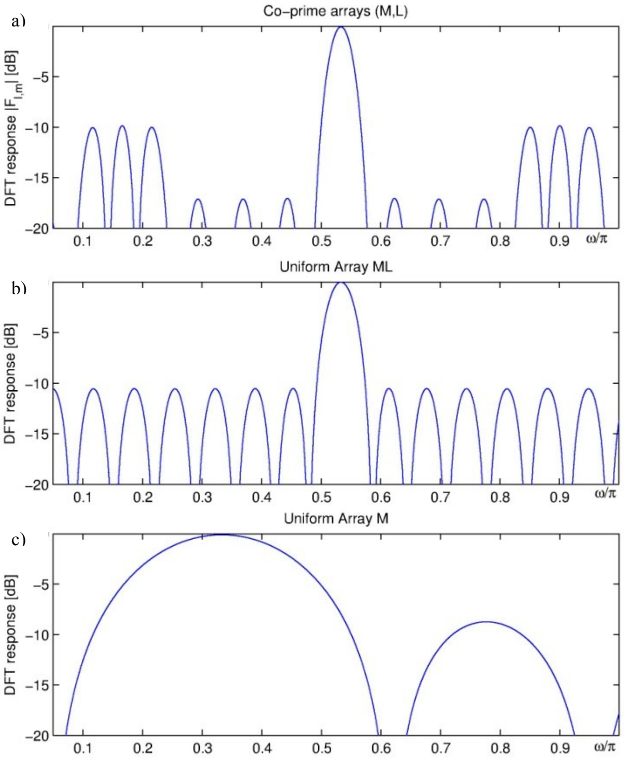

Fig. 3. A beam of: a) co-prime arrays with (M+L) elements (Fig. 3) and an ULA with: b) ML and c) M elements.

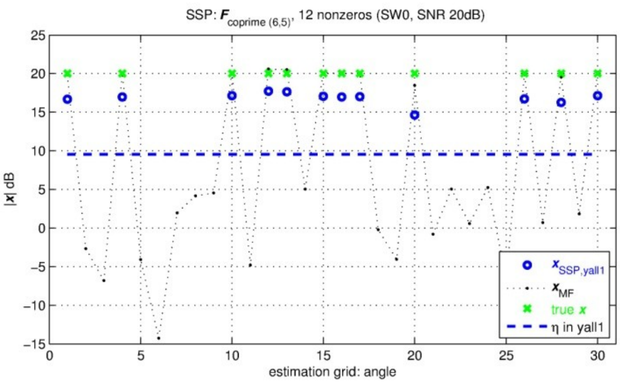

Fig. 4. SSP of 12 angles in a model from (5) .

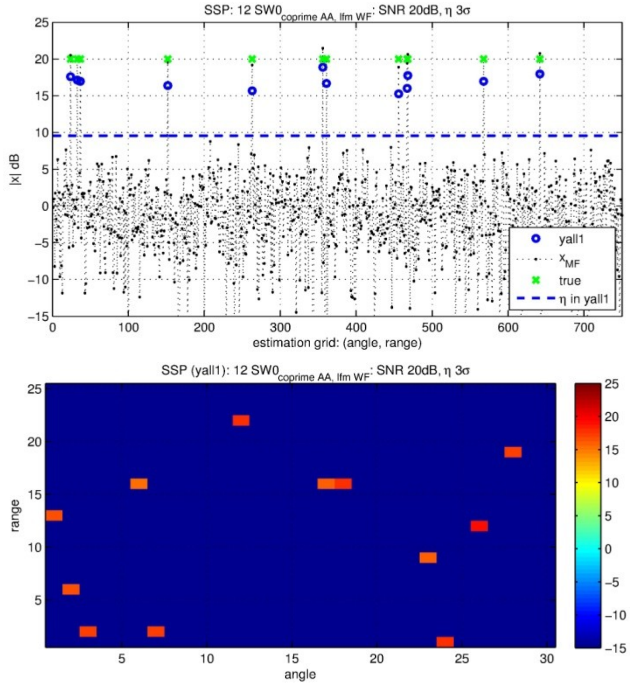

Fig. 5. SSP of 12 nonzeros in an angle-range profile (vector and matrix forms) in a model from (6) .

This angle-range processing demonstrates the potential of the co-prime LAs in CS radar whose optimal PG is feasible because spatial and temporal data are merged in $\boldsymbol{y}$, and used in SSP of a radar profile $\boldsymbol{x}$. The extension also enlarges the sparsity of such a radar profile because the same targets are looked in a larger parameter space.

4.2. Angular information distances from co-prime LAs

The advantages of the co-prime array solution are evident from beam widths when compared to ULAs with M and ML elements, as in Fig. 3. Besides the beams from 4.1, we also explore the whole potential angular resolution based on information distances in an azimuth-only case whose measurements are acquired from LAs, as explained in Section 3. In particular, since fewer measurements are acquired by co-prime arrays, we investigate differences in the possible angle resolution with co-prime arrays in comparison with the full ULA of size M and of size ML. For fair comparison of the PG effects, we let the transmit array as well as the target echo α be equal in all the three receive LA cases. Moreover, α is kept constant and equal to one, α = 1, so that the target (input) SNR can be ignored, SNR = $|\alpha|^2/\gamma$ = 1. The data model is common as given by (7) while LA configurations differ per case as:

- ULA M: $\{\mu_i\} = \{0\ 1\ ...\ M\text{-}1\}$;
- ULA ML: $\{\mu_i\} = \{0\ 1\ ...\ ML\text{-}1\}$; and
- co-prime (M,L) M *receive*: $\{\mu_i\} = \{0\ L\ 2L\ ...\ (M\text{-}1)L\}$.

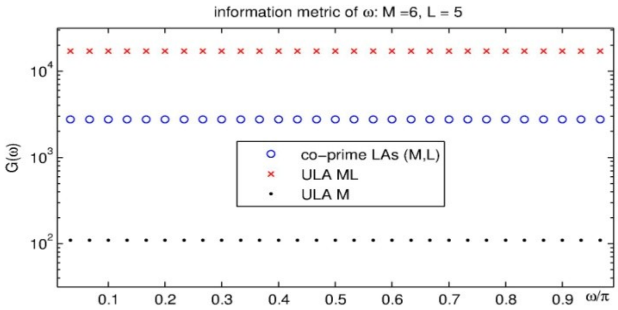

Fig. 6. Information metric $G(\omega)$ as defined in (8), and computed for three LA configurations, at SNR = 1.

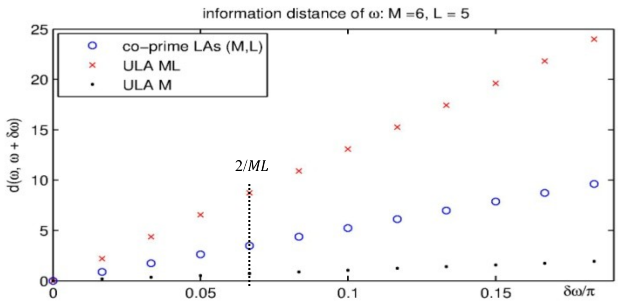

Fig. 7. Information distances as defined in (9), and computed with $G(\omega)$ from Fig. 6. Separation $\delta\omega/\pi$ of $2/ML$ is the DFT bin size indicating resolution from 4.1 and Fig.3a-b.

As expected, the full ULA with ML receive elements acquires the largest $G(\omega)$ (providing the best information resolution in ω) as obvious from Fig. 6 and Fig. 7 with results from the three LAs, M=6 and L=5 (as in Fig. 1). However, although having M receive elements only, the co-prime LAs perform fairly close to the full ULA with ML elements. The information distances (i.e. the potential high resolution) from the co-prime LAs are significant at small δω, as shown in Fig. 7. E.g. at the specific $\delta\omega/\pi$ of $2/ML$ (that is the DFT bin size in Fig. 3a-b) the information distance is 3.4960 as compared to 8.7203 of the full ULA. As given in (9), for the same information resolution, this is to be compensated by 6.22 times stronger SNR. This also holds for the accuracy given by $\mathrm{CRB}(\omega)$. Furthermore, co-prime LAs perform also much better than the full ULA with M receive elements. At the typical $\delta\omega/\pi$ of $2/ML$, the information distance is 3.4960 as compared to 0.6992 of the full ULA. This means that with the same number of receive elements, the co-prime LAs reaches the same information resolution with 25 times weaker SNR. Thus, regarding the angular information resolution, the co-prime LAs are much closer to the full ULA with ML elements than to the full ULA with M elements.

5. CONCLUSIONS

Potential angular resolution is crucial when using co-prime AAs that can be convenient for spatial sparse sensing in the front-end of a sensor with CS. In the back-end, the resolution potential is also relevant in SSP as it poses the limits to the SSP high-resolution performance.

Accordingly, we investigate not only the resulting beam width that depends on the AA configuration size, but also the effects of fewer measurements that are acquired by co-prime AAs. These PG effects can be seen in angular information resolution because it is computed from the intrinsic geometrical structure of data models that is characterized by the Fisher information.

Based on this information-geometry approach to angular resolution, we can conclude that active co-prime LAs with (M+L) elements perform much more closely to the full ULA with ML elements than to the full ULA with the same number M of receive elements. Moreover, we can also conclude that the concept of information resolution is appropriate for the resolution analysis in radar because of the completeness of the crucial effects it can take into account: the AA configuration and the input SNR.

5.1. Future work

In further work on information resolution, we will extend the analysis to all radar parameters: range, doppler and angle(s) in order to be able to resolve close targets in the whole parameter space. Moreover, while focusing on the system level, we will also explore the ease of achieving high resolution per parameter. Finally, we will keep designing the SSP estimation grid based on the information resolution what also involves proper sensing incoherence.

6. REFERENCES

[1] A. J. den Dekker and A. van den Bos, “Resolution: a survey", *Journal of the Optical Society of America A*, vol. 14, no. 3, 1997.

[2] E. de Jong and R. Pribić, “Sparse signal processing on estimation grid with constant information distance applied in radar”, *EURASIP Journal on Advances in SP,* 2014:78.

[3] S. Amari. "Information geometry of statistical inference - an overview", *IEEE* IT Workshop, pp. 86-89, 2002.

[4] S Kay, The geometry of statistical inference, in *Plenary at IEEE Workshop SAM* 2012.

[5] Y. Cheng, X. Wang, T. Caelli, X. Li and B. Moran, “On information resolution of radar systems", *IEEE Trans on AES*, vol. 48, no. 4, pp. 3084-3102, 2012.

[6] D. Donoho, “Compressed sensing,” *IEEE Trans. on IT*, vol. 52/no. 4, pp. 1289–1306, 2005.

[7] R. Pribić and I. Kyriakides, “Design of Sparse-signal processing in Radar Systems,” *IEEE* ICASSP 2014.

[8] H.L. Yap and R. Pribić, “False Alarms in Multi-Target Detection within a Sparsity Framework”, SEE Radar 2014.

[9] P.P. Vaidynathan and P. Pal, “Sparse Sensing With Co-Prime Samplers and Arrays”, *IEEE Trans. on SP*, vol.59/no.2, 2011.

[10] Y. Cheng, X. Wang, and B. Moran, “Angular Information Resolution Limit of Sensor Arrays", *IEEE SAM* 2014.

[11] D. D. Ariananda and G. Leus, “Compressive Joint Angular-frequency Power Spectrum Estimation”, *EUSIPCO 2013.*

[12] R. Pribić and L. Cifola. “Antenna-array Design in CS Radar Systems”, *CoSeRa 2015.*

[13] Y. D. Zhang, M. G. Amin and B. Himed, “Sparsity-based DOA estimation using co-prime arrays”, ICASSP 2013.

[14] Z. Tan, Y. C. Eldar, and A. Nehorai, “Direction of Arrival Estimation Using Co-Prime Arrays: A Super Resolution Viewpoint”, *IEEE Trans. on SP*, vol. 62/no. 21, 2014.

[15] C. E. Cook and M. Bernfeld. *Radar signals; an introduction to theory and application.* Academic Press, 1967.

[16] H. L. Van Trees. *Optimum Array Processing*. Wiley, 2002.

[17] yall1: your algorithms for L1, http://yall1.blogs.rice.edu/.